Journal of the European Ceramic Society **17** (1997) 289–297

PII: S0955-2219(96)00143-4
0955-2219/97/$17.00

Tape Casting of Alumina in Water with an Acrylic Latex Binder

Annika Kristoffersson & Elis Carlström

Swedish Ceramic Institute, Box 5403, 402 29 Göteborg, Sweden

(Received 15 September 1995; accepted 22 July 1996)

Abstract

Aqueous tape casting of alumina with an acrylic latex binder has been studied in a continuous tape casting machine. The aim of the study was to evaluate this type of system in the different processing steps. Four slurry compositions were used in the experiments with varied binder level and solids content. The rheological properties of the slips were measured with a controlled stress rheometer and related to the casting behaviour. The critical cracking thickness, i.e. the thickness when spontaneous cracking during drying occurs, was also studied. Casting rates of 2 cm/s resulting in a total drying time of 3·1 min could be used for slips with a high solids content at a blade gap of 300 μm. All slurries gave good quality tapes with smooth surfaces. The tapes were possible to laminate at room temperature. A bending strength of 536 MPa and a Weibull modulus of 17 were reached for a material laminated from 200 μm green tapes. © 1996 Elsevier Science Limited.

1 Introduction

Tape casting is a forming method that has mainly been used in the electronics industry to produce multi-layer capacitors and electronic substrates. New applications, in which thin layers formed by tape casting are used, are starting to appear. Flat ceramic membranes, solid oxide fuel cells, laminate composites for structural applications, transducers and actuators of piezoelectric ceramics are a few examples.

Tape casting has traditionally been performed using organic solvents as the liquid medium but there is now a trend to move away from organic solvents and an expected transition towards water-based systems.[1] The main advantage of a water-based system is that health and environmental risks can be reduced. A lower cost and a minimised explosion risk are other advantages. A major disadvantage that has been discussed is the expected slow drying rate when water is used as solvent.[2]

A wide range of water-soluble binders exists and several of these have been evaluated for tape casting.[3,4] Derivates of cellulose ethers[5,6] such as hydroxyethylcellulose and hydroxypropylmethylcellulose, polyvinyl alcohols,[7] acrylic polymers[8,9] and acrylic polymer emulsions, more commonly referred to as latex binders,[10,11] have been studied. In this paper we discuss the use of an acrylic latex binder for the tape casting of alumina. The study was directed towards the entire processing route from dispersing to sintering. The aim of the study was to examine the behaviour of this type of system in the different processing steps and to give an idea of the possibilities and limitations of this type of binder.

In tape casting it is desirable to have a process with a short processing time, process reproducibility, good economics and no environmental effects. The final product also has to meet specifications of reproducible high quality without detrimental defects. These requirements place specific demands on the different steps in tape casting.

In this study the production capacity of tape was investigated. Here the drying properties of the slurry are important because they limit the speed that can be used and what thickness range can be obtained.[12] The rheological properties of the slip were also studied with creep recovery, viscosity and oscillation measurements with a controlled stress rheometer. A stable slurry with appropriate rheological properties is desirable and a slurry with high solids content and pseudoplastic behaviour is favoured to give uniform tapes with high green density without segregation of the binder. The binder was evaluated with regard to the green density and the lamination behaviour of the tape. In the lamination, control of the plastic deformation in the different tape directions is important so that green density and sintering shrinkage can be controlled. Some plastic deformation, especially in the thickness direction, is desired

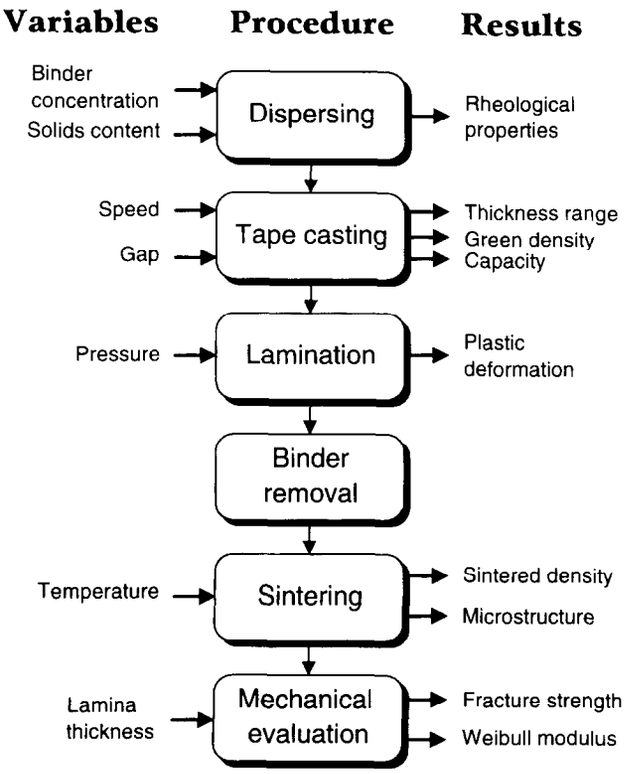

Fig. 1. Processing sequence for the experiments with used variables and results.

to accommodate, for instance, screen-printed electrodes and give good adhesion between the laminae layers. Binder removal experiments were performed to ensure a safe burn-out rate. Sintering experiments were made, in which the final density and shrinkage in different directions were evaluated. Finally, the mechanical properties such as bending, strength and Weibull modulus of the sintered materials were measured. In Fig. 1 the processing sequence for the experiments and the variables studied and their results are shown.

2 Experimental Procedures

2.1 Materials

An alumina powder (AKP 30, Sumitomo Chemicals) with an average particle size of 0·4 μm was used in this study. For dispersing, 0·3 wt% on Al_2O_3 powder of an ammonium salt of a polyacrylic acid (Dispex A40, Allied Colloids) was used. Hereby low-viscosity stable suspensions with high solids loading at pH around 9 are obtained. A copolymeric styrene-acrylic latex (Mowilith DM 765S, Hoechst Perstorp AB) was used as a binder. This is a nonionic latex, stable at neutral and basic pH, which makes it compatible with the alumina slurries. The latex is a dispersion with fine particles of 0·1–0·2 μm and a solids content of 50 wt%. The polymer film formed on drying has a glass transition temperature of −16°C, which makes it flexible and elastic at room temperature.

Four different slurry compositions were used in the experiments (Table 1). A high, 10 wt%, and a low, 7 wt%, binder level on alumina powder, and a high, 75 wt%, and a low, 67 wt%, solids content of the slurries were used. Batches of 1000 g alumina powder were dispersed in water by ball-milling for 18 h in 4-litre HDPE plastic jars with 2000 g of Si_3N_4 balls. After ball-milling, the latex binder was added and gently mixed for approximately 1 h. The slip was then sieved through a 31·5 μm cloth to remove agglomerates and entrapped air.

2.2 Rheological measurements

The rheological properties of these slips were characterised with a controlled stress rheometer (Stresstech Rheologica AB). First, viscosity was measured in a shear rate range from 0·04 s^{-1} to 462 s^{-1} in 13 logarithmic steps. This gives the flow behaviour and the viscosity level at both high and low shear rates. Another type of characterisation, creep recovery measurement, where the stresses are similar to those occurring during tape casting, was also used. During tape casting the slip is submitted to a stress that changes from a low level to a high level when the slip passes under the doctor blade. When the slip has passed the blade the stress is released. In the creep recovery measurements, the creep stress is increased to a certain level for the same time as it takes the slip to pass under the doctor blade. Then, the recovery response of the slip is measured until the stress level has reached a constant value. Three different stress levels, 5, 10 and 20 Pa, for a time of 0·3 s were used. Finally, the viscoelastic properties were measured with an oscillation stress sweep from the linear viscoelastic region to where the structure of the slip is broken down. The measurement was made at a frequency of 3 Hz and stress intervals from 0·026 to 3·00 Pa in 20 linear steps.

2.3 Tape casting

In the tape casting experiments, a continuous tape caster (TC 155 Wallace Technical Ceramics, Inc.) with a stationary casting head was used. The machine is specially designed for making thin tapes with a thickness range of 4–400 μm. The drying section is designed in such a way as to allow rapid drying and, at the same time, reduce the risk of skin formation and cracking. Heat is supplied from underneath the tape to improve the diffusion of solvent to the surface. At the same time, solvent is evaporated and transported by heated air which flows counter-currently to the tape. The result is a minimised risk of skin formation as the

Table 1. Slurry compositions used in the tape casting experiments

Designation	*Solids content*		*Binder/(binder + alumina)*		*pH*
	(wt%)	*(vol%)*	*(wt%)*	*(vol%)*	
Low 7	67·7	38·6	6·5	21·8	8·9
Low 10[a]	67·0 (67·1)	39·3 (39·9)	9·1	28·5	9·0 (8·6)
High 7	75·1	47·5	6·5	21·8	8·6
High 10[a]	74·6 (75·1)	48·4 (49·1)	9·1	28·5	8·9 (8·8)

[a]Two slurries of these compositions were prepared where the second was used for rheological characterisation. Their data are presented in parentheses.

drying air has been saturated with solvent vapour when it meets the wet film. The heat from underneath and the air flow can be balanced to make the rate of diffusion agree with the rate of evaporation. This makes the tape caster well suited for a water-based system in which the drying rates are generally lower compared with organic systems.

Tape casting experiments were made at speeds from 1 up to 5 cm/s with doctor blade gaps ranging from 100 to 500 μm. The drying conditions were the same in all experiments, the temperature of the heated sections was 50°C and the exhaust air 30°C. The air velocity was approximately 2 m/s, corresponding to an air flow of ~0·9 m^3/min. Steady state conditions were reached after only 1–2 min. The carrier film was a polypropylene plastic film of 60 μm thickness (WW-060, Western Wallis Co.).

One parameter in tape casting which is important to characterise is the critical cracking thickness, CCT.[12] This is the thickness at which the tape starts to give spontaneous cracking owing to shrinkage stresses during drying. This is especially true for water-based systems as the capillary forces during drying are higher than for systems in which organic solvents are used. This is a result of the high surface tension of water. The maximum capillary pressure during drying is related to the surface tension and the surface-to-volume ratio of the pore space, eqn (1).[13] This means that the capillary forces are inversely proportional to the pore volume, which means that the particle size and the particle size distribution of the powder influence the critical cracking thickness.

$$P_R = \frac{(\gamma_{SV} - \gamma_{SL})S_P}{V_P} \quad (1)$$

where, P_R = maximum capillary pressure, γ_{SV} = surface tension, solid/vapour, γ_{SL} = surface tension, solid liquid, and S_P/V_P = surface-to-volume ratio of pore space.

A method for checking the critical cracking thickness of the tapes has been developed. By setting the casting head to vary the gap width across the tape the critical cracking thickness can be checked. The blade width was 15 cm and two different gaps were used: 40–500 μm and 500–1000 μm. Figure 2 shows the casting station with a sloping gap and cracks in the dry tape at the CCT and above.

2.4 Lamination

In the lamination step, the plastic deformation in the different tape direction — thickness, casting direction and perpendicular to casting direction — was studied. Squares 57·5 by 57·5 mm were cut from the green tape and stacked to a height of at least 2 mm. These stacks were then pressed for 5 min at pressures between 12·1 and 60·5 MPa at room temperature.

2.5 Binder removal and sintering

Binder removal of green laminates was made at a constant temperature rate of 1°C/min to 500°C in air. Experiments in which the binder removal rate was controlled by the weight loss were also performed to decrease the time needed for binder removal. Laminated plates of the *High 10* composition were sintered at temperatures between

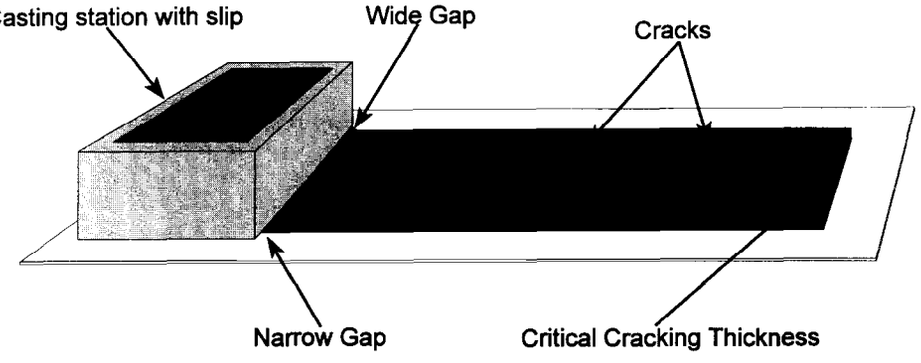

Fig. 2. Casting station with sloping gap for checking the Critical Cracking Thickness, CCT.

1400°C and 1600°C for 1 h and a heating rate of 10°C/min. A sintering temperature of 1550°C was chosen for the materials for mechanical testing.

2.6 Mechanical testing

The fracture strength was measured in four-point bending for the *High 7* and *High 10* compositions laminated at 60·5 MPa. Plates made up from tapes cast at 300 and 150 μm blade gap were used to study the influence of lamina thickness on the fracture strength and Weibull modulus. This was done to check the lamination step and to see if a limit in defect size can be obtained by limiting the tape thickness. The resulting thicknesses of the tapes were approximately 200 and 100 μm for the *High 7* composition, and 140 and 80 μm for the *High 10* composition. Test bars with dimensions of 3·0 × 4·0 × 50 mm^3 were cut from sintered, ground plates. The test bars were chamfered before testing. The samples were tested in four-point bending with a 40/20 mm rig and a loading rate of 1·0 mm/min.

3 Results and Discussion

3.1 Rheological measurements

The rheological properties of the four slips were characterised by viscosity, creep recovery, and oscillation measurements.[14] The results of these measurements are summarised in Table 2. The viscosity was measured over a shear rate interval from 0·04 to 462 s^{-1} and the resulting flow curves are shown in Fig. 3. All four slips displayed a pseudoplastic behaviour. As can be seen in the diagram, the viscosity level is largely influenced by the solids content but also by the amount of binder in the slips. Both the degree of pseudoplasticity and the viscosity increase with increasing solids content and binder ratio.

Figure 4 shows two examples of creep recovery measurements at 5 and 20 Pa for 0·3 s for the *High 10* slip. In a creep recovery measurement a shear stress is applied for a short time (the creep phase). The first curve (Fig. 4(a)), *High 10* at 5 Pa, illustrates a slip which has a viscoelastic response and partly behaves as a solid material while the second curve (Fig. 4(b)) shows the slip when the

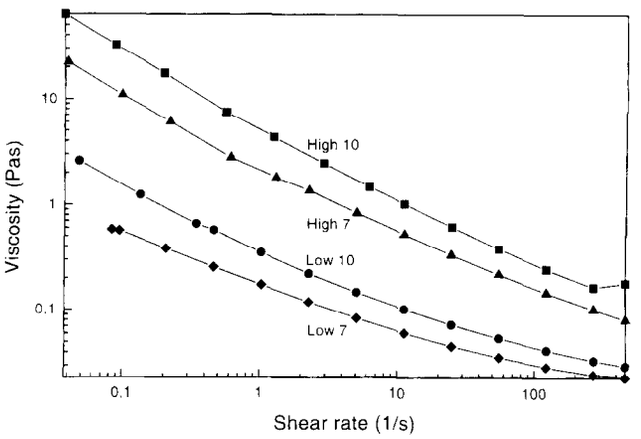

Fig. 3. Resulting flow curves of viscosity vs the shear rate.

stress at 20 Pa has exceeded the structural forces within the slip and the slip deforms as a pure liquid. Of the four slips, *High 10* was the only one which had a partly elastic response. The other three slips gave a viscous response at all three stress levels: 5, 10 and 20 Pa. The degree of elastic response of *High 10* decreases with increasing stress level. The time for which a slip is submitted to a certain stress level also influences the flow behaviour; a longer time at creep gives a larger deformation and more time to break down structures within the slip. The creep recovery measurement differs from viscosity measurements in the respect that viscosity measurements are made when equilibrium has been reached while creep recovery measurements measure transient effects. Creep recovery measurements could also be combined with pre-shearing simulating stirring and different times at rest after shearing, e.g. to study thixotropic effects.

Figure 5 shows an example of an oscillation stress sweep for the *High 10* and *Low 7* compositions. At low stresses we have the linear viscoelastic region where the moduli are constant. When the stress increases, the elastic part decreases and the overall complex modulus decreases. At a phase degree of 45° the storage modulus and the loss modulus have the same value, and if the shear stress is increased beyond this point, the slip behaves in a more viscous fashion. Values of the moduli and phase degree from the linear viscoelastic region are presented in Table 2 together with

Table 2. Summary of results from the rheological measurements of the four slurries

Slip	*Viscosity (mPas) Shear rate,*		*Data from linear viscoelastic region*		*Strain and type of flow from creep test for 0·3 s at a stress of,*	
	11·2 s^{-1}	*462 s^{-1}*	*G' (Pa)*	*Phase (°)*	*5 Pa*	*20 Pa*
Low 7	60·6	23·1	3·94	26·5	2·46, viscous	1·91, viscous
Low 10	101	29·7	8·04	22·5	2·47, viscous	1·73, viscous
High 7	522	80·2	43·0	11·2	1·64, viscous	1·91, viscous
High 10	1020	128	77·8	8·06	0·39, viscoelastic	2·15, viscous

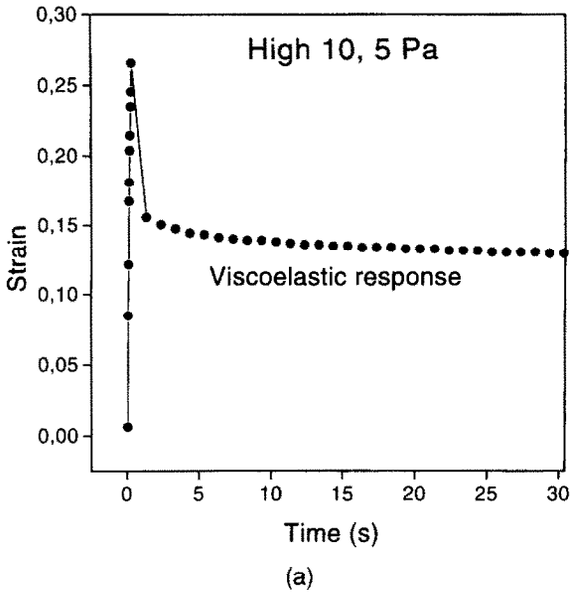

(a)

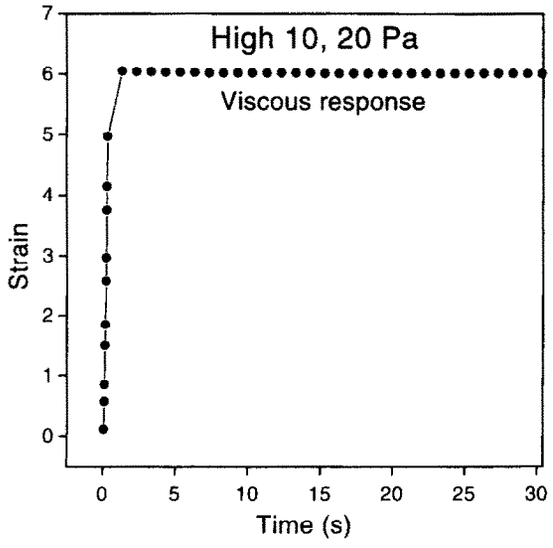

(b)

Fig. 4. Creep recovery measurements for the *High 10* slip at (a) 5 and (b) 20 Pa for 0·3 s.

values from the other measurements. As can be seen in the table and in agreement with earlier viscosity results, the slips exhibit a more elastic behaviour with an increased solids content and binder ratio. With only relatively small variations in compositions, the rheological properties vary significantly. Although the rheological properties varied to such a great extent all the slips were possible to use for tape-casting.

3.2 Tape casting

In the tape casing experiments the production capacity of tape was studied. Tapes were cast at 150 and 300 μm blade gaps and a casting rate of 2 cm/s for all the four slurries. The total drying time of the tapes at this speed before they are wound onto the storage reel is 3·1 min. At this

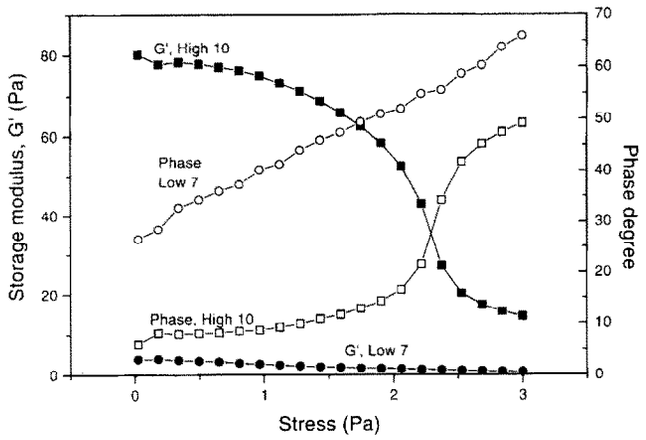

Fig. 5. Oscillation stress sweep from 0·026 to 3·0 Pa at 3 Hz for the *High 10* and *Low 7* slips.

speed and the drying conditions mentioned earlier, the tapes from slurries with a high solids content were completely dry when they reached the storage reel while tapes at a 300 μm gap with low solids content had to be cast at a lower speed — 1 cm/s — to be completely dry. The maximum casting speed tested on the *High 10* composition with a 150 μm gap was 11·7 cm/s. At this speed small bare spots occurred but good quality tape could be cast with this composition at 5 cm/s. In all of these experiments the casting rates were relatively high and the drying time short, which helps to minimise the risk of binder/powder segregation. The high production capacity of this water-based system is a result of high solids loading in combination with the heating from underneath and heated air, enabling a short drying time. The casting rates used in these experiments are similar to those reported in literature for other water-based systems,[2,6] but in these continuous tape casters were used and the total drying time was longer. No data on drying times and casting rates when using continuous tape casters and water-based systems have been found in literature. Typical continuous tape casters can operate at speeds from 0·2 to 15 cm/s where the high casting rates are used for thin tapes. The casting rate used in a continuous tape caster depends on the length of the drying section. With a longer drying section a higher casting rate can be used.

All of the slurries gave good quality tapes with smooth surfaces without blisters or pin-holes. The green tapes were easy to release from the carrier film, flexible and easy to handle. All of the slurries wetted the polypropylene carrier film to a sufficiently high degree without extra addition of surfactants. However, full wetting of the carrier film is not necessary because the drying front of the drying layer in a continuous tape caster 'locks' the tape and inhibits the slip from receding and forming drops.

The thickness range was another variable studied. The minimum thickness that could be obtained was governed by the tape's release from the carrier film. Tapes with 25 μm thickness were cast and released from the carrier film. Thinner tapes were cast but these were difficult to release from the carrier film. The maximum thickness that can be reached is limited by cracking due to stresses occurring during the drying stage. A sloping gap was used to check the CCT of the four slurry compositions. The method with a sloping gap for checking the CCT was verified to agree with the critical cracking thickness that was obtained with a normal parallel gap set to different thicknesses for SiC slips. The majority of cracks occurred perpendicular to the casting direction with a few cracks running between these cracks parallel to the casting direction. This is probably a result of constraint by the carrier film in both directions but more pronounced in the tape direction. Over a certain distance from wet layer to dry tape we have a moisture gradient as drying proceeds and shrinkage starts. This, together with the constraint by the carrier film and the capillary pressure, give stresses that cause cracking at a critical cracking thickness.[12] The results are presented in Table 3 together with the green density and finished film thickness.

CCT in the 400 μm region was reached for the slips with high solids content. This can be compared with the reported CCT over 175 μm and above for binder-free alumina slips, AKP 30, 20 vol% dried slowly over 48 h.[12] In the literature, tape thicknesses in the 150–300 μm region have been reported for aqueous systems with latex binders.[2,10,11] However, these were tape cast in non-continuous tape casters using longer drying times. No exact CCT of the *Low 7* and *Low 10* compositions could be specified as thicker layers of these slips start to flow in the sloping drying section because of low viscosity and they were not sufficiently dry at this point when a casting rate of 1 cm/s was used. The lower CCT of the composition with more binder, *High 10* compared with *High 7*, is probably due to the larger capillary forces in the *High 10* composition with more, smaller particles. A higher CCT could have been expected with a higher binder ratio but the latex does not act as a binder until it has coalesced fully upon drying, and cracking occurs before this stage. The latex binder might have both a negative and a positive influence on the CCT compared with other water-based binders. A low viscosity at a high polymer concentration enables high solids loaded slips resulting in a high CCT, while a latex does not hinder cracking (act as a binder) until a film has formed, decreasing the CCT. The green densities increase with increased solids content and decreased binder ratio. These results are similar to those reported in the literature.[6,11] For lower solids loading, more rearrangement of particles and binders is needed from the wet to dry stage. In the short drying period full rearrangement is not possible, while in the higher solids loading slips the powder and binder are better packed from the start. The same type of effect is probably responsible for the difference in density with binder content; more binder hinders an optimum packing.

The casting rates of 1 and 2 cm/s correspond to shear rates of 33 and 67 s^{-1}. If the slips are suddenly submitted to this shearing after very low shear they give a viscous or a viscoelastic response depending on whether the stress is sufficient to break down the structure present within the slip. For the low-viscosity slips a relatively low stress, <5 Pa, is needed to give a pure viscous response in the creep recovery measurements. This was also verified in the viscosity measurements where a lower stress was needed to reach a certain shear rate at a lower viscosity level. During casting this stress was exceeded and the tape thickness was virtually unaffected by the casting speeds tested in these experiments. For the *High 10* slip with the most elastic behaviour the casting speed strongly influenced the cast thickness. At a low speed thinner tapes were obtained, probably as a result of the low shear rate and the corresponding stress not being high enough to give viscous flow. At the higher speed, 2 cm/s, a higher shear rate, and higher stress, a thicker tape was reached as a result of better flow behaviour at a lower viscosity. The stress profile under the blade probably varies with the viscous or viscoelastic behaviour, resulting in a steeper profile for a viscoelastic

Table 3. Green density, critical cracking thickness and tape thickness of the four compositions

Slip	*Green density (less the binder)*		*Critical cracking thickness*	*Tape thickness, dry and wet[a] cast at a 300-μm gap and a speed of*			
	(g/cm³)	*(%)*	*(μm)*	*1 cm/s*	*(μm)*	*2 cm/s*	*(μm)*
Low 7	2·01	50·5	>300	141	(239)	142	(241)
Low 10	1·96	49·3	>290	138	(240)	139	(242)
High 7	2·04	51·1	410	170	(233)	168	(230)
High 10	2·00	50·3	370	136	(194)	168	(240)

[a]Values in parentheses represent the wet thickness calculated from green density and solids content.

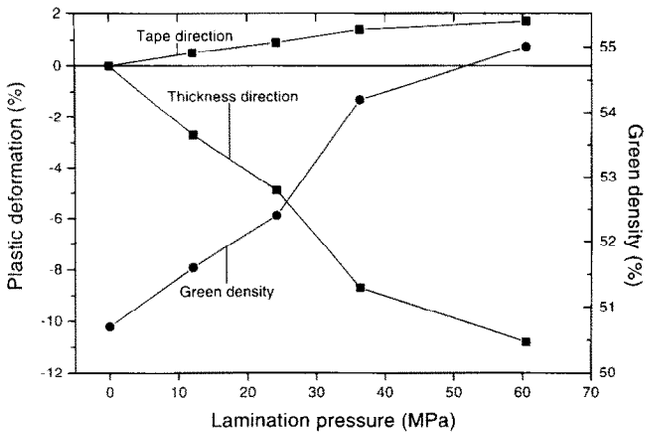

Fig. 6. Plastic deformation and resulting green density as a function of lamination pressure for green tapes of *High 10* composition.

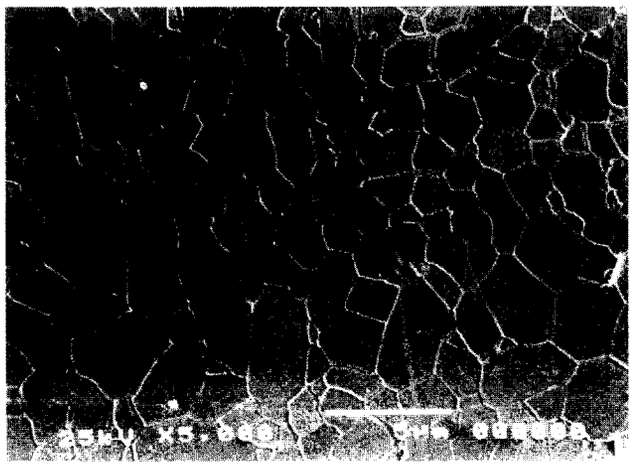

Fig. 7. Microstructure of *High 10* sintered at 1550 °C.

behaviour. The effects of casting speed on thickness in relation to the rheological properties of the slips require further studies over a wider range of casting speeds especially for non-Newtonian slips. This is especially important for water-based systems when the solids content is maximised resulting in non-Newtonian slips. A flow model has been proposed for tape casting,[15] but in this flow model a Newtonian flow was assumed.

3.3 Lamination

The plastic deformation during lamination was studied on green tapes of the *High 10* composition. No difference in plastic deformation between the casting direction and the direction perpendicular to casting was observed. Most of the plastic deformation was in the thickness direction, as can be seen in Fig. 6.

In the lamination the green density increased from 50·3 to 55·0% relative density at a pressure of 60·5 MPa with the major part of the plastic deformation in the thickness direction of the *High 10* composition. For comparison the green density of *High 7* increased from 51·1% to 54·7% at a pressure of 60·5 MPa. All tapes were easy to handle and laminate at room temperature without the addition of a plasticiser owing to the low T_g of the latex.

3.4 Binder removal and sintering

Binder removal experiments were performed to ensure a safe burn-out rate. At a heating rate of 1°C/min up to 500°C in air the binder is pyrolysed without causing any problems such as deformation or blisters. The acrylic-styrene copolymer starts to decompose at 220°C followed by a second peak at 320°C and a final peak at a temperature of 450°C. When the weight loss of the binder was controlled and set to 1·1% of total binder content/min, and a heating rate of 5°C/min when the weight loss was lower than 1·1%, the total time for binder removal could be reduced to 3·0 h compared with 8·3 h in the experiment with a constant heating rate.

Laminated plates were test sintered at temperatures between 1400°C and 1600°C. A temperature of 1550°C was chosen at which the materials sintered to more than 99% relative density. (At a sintering temperature of 1600°C substantial coarsening of the grain structure was evident and lower temperatures, 1500°C and 1400°C, did not reach densities over 99%.) No difference in shrinkage between the different tape directions, casting direction and perpendicular to the casting direction, was observed after sintering. After sintering the single layers making up the laminate could not be distinguished. Figure 7 shows the microstructure of a sintered laminate.

3.5 Mechanical properties

The fracture strength was measured on materials sintered at 1550°C. Plates were laminated from tapes cast of the *High 7* and *High 10* compositions at blade gaps of 150 and 300 μm. The resulting fracture strengths and Weibull moduli are shown in Table 4.

The highest mechanical strength was obtained for the *High 7* composition laminated from 200 μm green tapes, 536 MPa and a Weibull modulus

Table 4. Fracture strength and Weibull modulus of *High 7* and *10* laminates

Material	*Green tape thickness (μm)*	*Fracture strength four-point (MPa)*			*Weibull modulus*
		Minimum	*Mean*	*Maximum*	
High 7	100	414	523	572	13·3
High 7	200	468	537	585	16·7
High 10	80	345	486	577	7·5
High 10	140	344	475	591	6·4

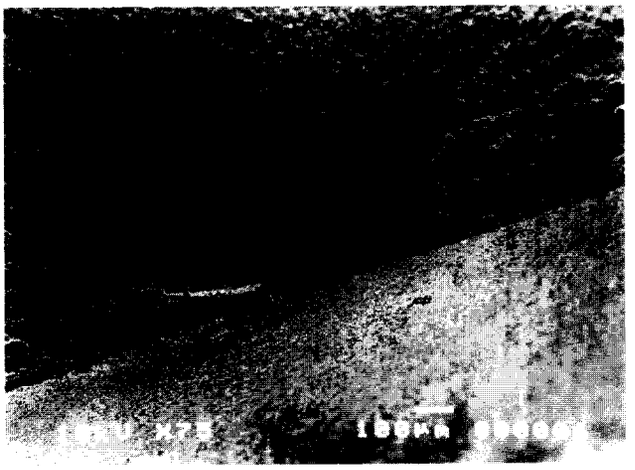

(a)

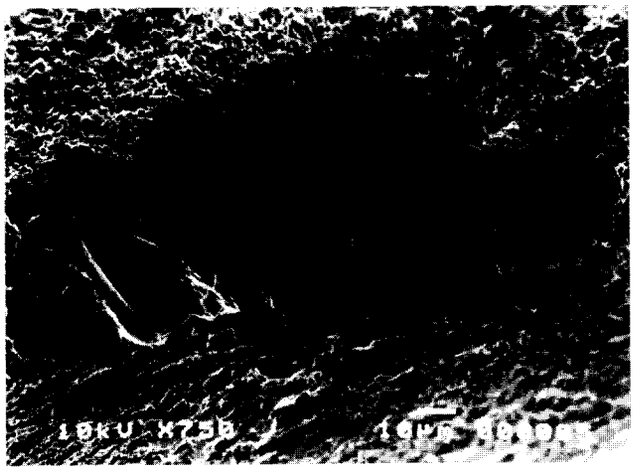

(b)

Fig. 8. Fractograph of a *High 10* test bar with fracture strength of 344 MPa where the failure cause is a large alumina grain.

of 17 (four-point bend with 40 mm span). With thinner green tapes, 100 μm, the strength dropped to 523 MPa and a modulus of 13. The *High 10* composition with thinner tapes reached a strength of 480 MPa and a substantially lower Weibull modulus of approximately 7. This is in agreement with results by Ham-Su[16] who showed that the Weibull modulus decreased with the number of layers in the laminate, i.e. the lamination does not give flaw elimination but is a possible step where defects can be introduced. Fractography was carried out to find the failure cause responsible for the difference in strength and especially Weibull modulus between the *High 7* and the *High 10* compositions. For the low-strength test bars of the *High 10* composition the failure cause was single, large grains or a group of large grains up to 100 μm in diameter. Figure 8 shows an example of one of these large grains found as failure cause of the low-strength test bars of the *High 10* composition. These types of defect were not found in the *High 7* composition. For strong test bars of both compositions the failure cause was pores. In the *High 10* composition a higher degree of inhomogeneous porosity was found. The reason for this is unclear but might be a result of the higher binder level. A higher binder level might make it more difficult for entrapped air between green layers to be dissipated in the lamination step. Inhomogeneous porosity may also promote exaggerated grain growth.

4 Conclusions

Stable slips of alumina and a nonionic acrylic latex binder were obtained at all the compositions and gave smooth, good quality tapes. High casting rates could be used thanks to the possibility of using high solids content slips and heating from underneath in the tape caster. Casting rates exceeding 2 cm/s resulting in a total drying time of 3·1 min or less could be used for both the slips with high solids content, 48 vol%, at a blade gap of 300 μm. A method for checking the critical cracking thickness, CCT, has also been developed. The CCT was approximately 400 μm for slips with high solids content. The rheological properties, especially the degree of pseudoplasticity and degree of viscoelastic behaviour, increased significantly with binder ratio and solids content. In the studied range, the finished tape thickness from slips with viscous behaviour was virtually unaffected by the casting rate while the finished tape thickness was strongly influenced by the casting rate for slips with viscoelastic behaviour. This is believed to be related to the viscous or viscoelastic behaviour at the shear stress given under the doctor blade during casting. The green sheets could be laminated at room temperature owing to the low T_g, −16°C, of the latex. The highest measured bending strength was 536 MPa with a Weibull modulus of 17.

Acknowledgements

The authors would like to thank the Swedish National Board for Industrial and Technical Development (Nutek) for the financial support. The authors would also like to thank Margareta Jansson for preparing this manuscript.

References

1. Mistler, R. E., Tape casting: The basic process for meeting the needs of the electronics industry. *Am. Ceram. Soc. Bull.*, **69** (1990) 1022–1026.

2. Nahass, P., Rhine, W. E., Pober, R. L. & Bowen, H. K., A comparison of aqueous and non-aqueous slurries for tape-casting, and dimensional stability in green tapes. In *Ceramic Transactions,* Vol. 15, *Materials and Processes for Microelectric Systems*, eds K. M. Nair, R. Pohanka & R. C. Buchanan. The American Ceramic Society, 1990, pp. 355–364.
3. Moreno, R., The role of slip additives in tape casting technology: Part II — Binders and plasticizers. *Am. Ceram. Soc. Bull.*, **71**(11) (1991) 1647–1657.
4. Onoda Jr, G. Y., The rheology of organic binder solutions. In *Ceramic Processing before Firing*, eds G. Y. Onoda Jr & L. L. Hench. John Wiley, New York, 1978, pp. 235–251.
5. Burnfield, K. E. & Peterson, B. C., Cellulose ethers in tape casting formulation. In *Ceramic Transactions,* Vol. 26, *Forming Science and Technology for Ceramics*, ed. M. J. Cima. The American Ceramic Society, 1992, pp. 191–196.
6. Chartier, T. & Bruneau, A., Aqueous tape casting of alumina substrates. *J. Eur. Ceram. Soc.*, **12**(4) (1993) 243–247.
7. Raeder, H., Glenne, R. & Simon, C., Water based tape casting of yttria-stabilised zirconia: Influence of powder properties. Presented at the Powder Processing and Technology Conference at Friedrichshafen, Germany, Sept. 1994 (to be published).
8. Nagata, K., Correlation of conformation of acrylic polymers in aqueous suspensions and properties of alumina green sheets. In *Ceramic Transactions,* Vol. 26, *Forming Science and Technology for Ceramics*, ed. M. J. Cima. The American Ceramic Society, 1992, pp. 205–210.
9. Galassi, C., Rastelli, E., Roncari, E. & Basile, F., Characterization of water based tape casting slurries. In *Proceedings of Eighth Cimtec World Ceramics Congress, Ceramics: Charting the Future, Part C*, ed. P. Vincenzini. Techna srl, 1995.
10. Gurak, N. R., Josty, P. L. & Thompson, R. J., Properties and uses of synthetic emulsion polymers as binders in advanced ceramic processing. *Am. Ceram. Soc. Bull.*, **66** (1987) 1495–1497.
11. Ushifusa, N. & Cima, M. J., Aqueous processing of mullite-containing green sheets. *J. Am. Ceram. Soc.*, **74** (1991) 2443–2447.
12. Chiu, R. C., Garino, T. J. & Cima, M. J., Drying of granular ceramic films: I. Effect of processing variables on cracking behaviour. *J. Am. Ceram. Soc.*, **76** (1993) 2257–2264.
13. Scherer, G. W., Theory of drying. *J. Am. Ceram. Soc.*, **73** (1990) 3–14.
14. Barnes, H. A., Hutton, J. F. & Walters, K., *An Introduction to Rheology*, 1st edn. Elsevier, Amsterdam, 1989.
15. Chou, Y. T., Ko, Y. T. & Yan, M. F., Fluid flow model for ceramic tape casting. *J. Am. Ceram. Soc.*, **70** (1987) C-280–282.
16. Ham-Su, R. & Wilkinson, D. S., Strength and flaw elimination assessment in tape cast ceramic laminates. In *Ceram. Eng. & Sci. Proc.*, **13**(9–10), The American Ceramic Society, 1992, pp. 1000–1007.